FOR THE RECORD

Discovery of a significant, nontopological preference for antiparallel alignment of helices with parallel regions in sheets

BRANDON M. HESPENHEIDE AND LESLIE A. KUHN

Department of Biochemistry and Molecular Biology and Center for Biological Modeling, Michigan State University, East Lansing, Michigan 48824, USA

(RECEIVED November 11, 2002; FINAL REVISION January 31, 2003; ACCEPTED February 17, 2003)

Abstract

To help elucidate the role of secondary structure packing preferences in protein folding, here we present an analysis of the packing geometry observed between α-helices and between α-helices and β-sheets in 1316 diverse, nonredundant protein structures. Finite-length vectors were fit to the α-carbon atoms in each of the helices and strands, and the packing angle between the vectors, Ω, was determined at the closest point of approach within each helix–helix or helix–sheet pair. Helix–sheet interactions were found in 391 of the proteins, and the distributions of Ω values were calculated for all the helix–sheet and helix–helix interactions. The packing angle preferences for helix–helix interactions are similar to those previously observed. However, analysis of helix–strand packing preferences uncovered a remarkable tendency for helices to align antiparallel to parallel regions of β-sheets, independent of the topological constraints or prevalence of β-α-β motifs in the proteins. This packing angle preference is significantly diminished in helix interactions involving mixed and antiparallel β-sheets, suggesting a role for helix–sheet dipole alignment in guiding supersecondary structure formation in protein folding. This knowledge of preferred packing angles can be used to guide the engineering of stable protein modules.

Keywords: Protein folding; secondary structure packing; folding cores; helix and sheet dipoles; protein design; diffusion–collision model

The mechanism by which a protein folds from a denatured state to a folded conformation is an intensely studied, unsolved problem in the natural sciences, although there are many studies presenting a partial solution (for reviews, see Bryngelson et al. 1995; Honig 1999; Baker 2000). Many models describing the folding reaction have been proposed and supported by experimental evidence, and a single model may not hold for all proteins. In one particular folding model, known as the framework (Udgaonkar and Baldwin 1988) or diffusion–collision model (Karplus and Weaver 1994), a subset of secondary structure elements forms partial or complete structure early in the folding reaction. These substructures interact, forming a supersecondary structure that is representative of the folding transition state ensemble, and folding then continues to the native state. For instance, both mutagenesis (Kippen et al. 1994) and hydrogen-deuterium out-exchange (H-D exchange) experiments (Perrett et al. 1995) have shown the framework model to be a valid scenario for the folding of barnase, in which the N-terminal α-helix packs against several strands of the C-terminal β-sheet to form an intermediate structure along the folding pathway. Analysis of protein folding for a series of other proteins, by hydrogen-exchange nuclear magnetic resonance spectroscopy (NMR) and computational approaches, indicates that the packing of two secondary structures forms a folding core that builds up to the native structure (Hespenheide et al. 2002; Li and Woodward 1999).

Reprint requests to: Leslie A. Kuhn, Michigan State University, 502C Biochemistry, East Lansing, MI 48824, USA; e-mail: kuhn@agua.bch.msu.edu; fax: 517-353-9334.

Article and publication are at http://www.proteinscience.org/cgi/doi/10.1110/ps.0238803.

Assuming the framework model is one valid scenario for protein folding, we can ask whether secondary structures prefer to adopt specific geometries when they coalesce. In one of the earliest studies on secondary structure packing, Chothia et al. (1981) analyzed 50 helix–helix packing interactions from 10 protein structures. The results led them to propose the "ridges into grooves" model, in which helix pairs adopt specific geometries allowing the side chains to interdigitate. Since that time, advances in computer technology have allowed for not only an invaluable increase in the number of protein crystal structures, but also the development of algorithms that allow the removal of statistical bias in the Protein Data Bank (PDB; Berman et al. 2000) toward protein families with many occurrences. More recent studies have expanded the analysis of helix–helix packing interactions to a dataset of 1776 interactions from 757 protein structures with <30% sequence identity and better than 2.4 Å resolution (Walther et al. 1998).

In studies of secondary structure packing, the secondary structures are often represented by best-fit lines through the C_α coordinates of the residues. A spherical–polar coordinate system is then used to measure packing geometries. For a pair of interacting structures, the geometry can be described by a single dihedral angle, referred to as Ω, formed by each structure and the line of closest approach between them (Fig. 1). Observed distributions of Ω packing angles for helix–helix interactions initially exhibited distinct peaks (Walther et al. 1996). However, Bowie (1997), with further developments by Walther et al. (1998), demonstrated that the expected uniform random distribution of Ω is actually biased toward angles near 90°. When this geometric bias was taken into account, the observed peaks in the helix–helix Ω angle distribution were significantly attenuated.

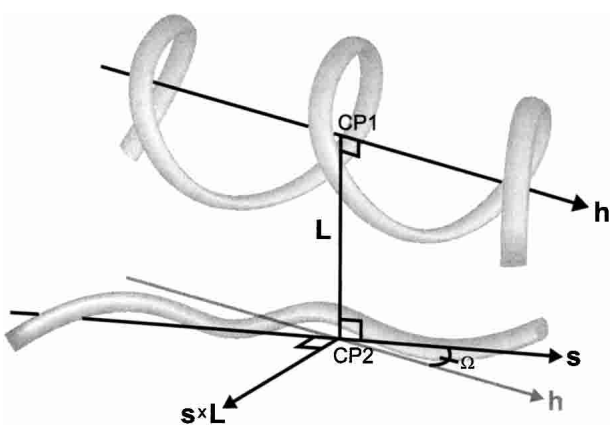

Figure 1. Graphical representation of a helix–sheet packing geometry. The helix and the strand are shown as light gray ribbons. The vector representations of the helix, **h**, and the strand, **s**, are shown as black arrows. The vector of closest approach, **L**, intersects the helix at a point labeled CP1, and the strand at the point CP2. Because **L** is perpendicular to **s**, their cross product, $\mathbf{s} \times \mathbf{L}$ is perpendicular to both. The Ω packing angle is measured as the angle between **s** and the projection of **h**, shown as a light gray arrow, onto the plane defined by axes **s** and $\mathbf{s} \times \mathbf{L}$.

Measuring the packing geometry for helix–sheet interactions has proven a difficult task because of the nonplanar nature of most β-sheets. Early work by Janin and Chothia (1980) stated that the Ω angle for a helix packing against a sheet should be near 0°, indicating that only small angles allowed for complementary packing of the helix side chains within the surface created by a β-sheet. This observation of helix–strand axial alignment was further supported by work published by Cohen et al. (1982) a few years later. A theoretical study in which low energy helix–sheet conformations were predicted also agreed that a helix–strand packing Ω angle near 0° was a favorable interaction (Chou et al. 1985). Their analysis of 163 helix–sheet packing interactions observed from proteins of known structure showed a predominant peak near 0°. In all of these studies, the packing angles were measured by approximating inherently twisted β-sheets as a plane. Also, the Ω angle was measured in the range $-90° \leq \Omega \leq 90°$; therefore, the N-terminal to C-terminal orientation of the secondary structures was not taken into account.

In this work, further analysis of helix–helix and helix–strand packing interactions is presented. The distribution of helix–helix Ω angles is found to be very similar to the data presented by Walther et al. (1998). For examining helix–sheet interactions, the strands in the sheet are categorized according to five possible orientations, depending on the direction of the strand relative to its neighbors (parallel versus antiparallel). The observed distribution of Ω packing angles is then presented, with geometric bias taken into account, for each of the five cases. The Ω packing angle for both helix–helix and helix–sheet interactions is measured over the range $-180° \leq \Omega \leq 180°$ to observe any correlation between parallel/antiparallel packing and Ω angle. A unique coordinate transformation is used to measure the Ω packing angle, so that an inherently twisted β-sheet is not approximated as a plane. The results indicate a strong preference for a helix to pack antiparallel (with Ω near ±180°) to a sheet composed of parallel strands. This preference is not dependent on the topological constraints imposed by short loops in β-α-β motifs (Sternberg and Thornton 1976), as the Ω angle distributions do not change significantly when β-α-β motifs are excluded from the dataset.

Results

Helix–helix packing angle distribution

The packing geometry of helix–helix pairs has been extensively studied in the past (Chothia et al. 1981; Reddy and Blundell 1993; Walther et al. 1996, 1998; Bowie 1997) and is included here mainly to assess any effects from increasing

the database size, and for validation purposes. The distribution of helix–helix Ω packing angles in our dataset is shown in Figure 2. This distribution is quite similar to the one presented in Walther et al. (1998), which previously had the most extensive dataset. Both parallel (Ω near 0) and antiparallel (Ω near +/− 180) helix–helix alignments are preferred.

Helix–strand Ω packing angle distribution as a function of strand orientation

For each helix–strand packing interaction, the strand can be in one of five orientations depending on whether it is parallel or antiparallel to its neighbors, and whether or not it is the first or last strand in the sheet (Table 1). The distributions of observed Ω packing angles for each strand orientation are presented in Figure 3A as the number of observed orientations divided by the number expected from a uniform random distribution for each 10° bin in Ω values. A value of 1.0 indicates that the range of observed Ω angles occurred just as often as expected. Values <1.0 represent unfavored Ω angles, and values >1.0 indicate preferred packing angles. Ω angles in the range $-90° < \Omega < 90°$ represent an interaction in which the N-terminal to C-terminal direction of the helix is parallel to the direction of the strand. For $\Omega < -90°$ or $\Omega > 90°$, the helix is packed antiparallel to the strand.

The presence of short loops between an interacting helix and strand could influence the observed Ω distribution by disallowing parallel packing interactions. To account for this, we analyzed a subset of the interactions shown in Figure 3A in which any helix–strand pair in which the helix and strand were consecutive secondary structures along the chain was excluded from the analysis, ensuring that the observed Ω angle did not arise from connectivity constraints. The Ω distributions for this set are shown in Figure 3B. Comparison of panels A and B shows a striking resemblance, indicating that the observed preference for helices to pack antiparallel to parallel regions of sheets is not an artifact of conformational constraints imposed by short loops between the interacting helix and strand.

Type −1 and −2 strand orientation distributions in both Figure 3A and 3B show some preference for parallel packing when the neighboring strands are antiparallel. Also, there is a preference to pack at angles near −30° and 150°, and to avoid packing at angles near −100° and +70°, similar to helix–helix packing. The top three panels in Figure 3 show that for parallel (type 0, 1, and 2) strand orientations, there is an increasing preference with increase in sheet parallelicity for the helix to pack antiparallel to the strand. Ω angles >90° are favored, whereas angles between −90° and +90° are disfavored. Type 2 strand orientations exhibit the strongest preference, with antiparallel packing strongly preferred, and almost no packing interactions observed in which the helix is oriented parallel to the strand. Figure 4 shows an ideal type 2 antiparallel helix–strand interaction present in the protein IIB cellobiose from *Escherichia coli* (PDB code: 1iib; van Montfort et al. 1997). The yellow arrows, representing β-strands, point in the N- to C-terminal direction. The N- to C-terminal direction of the helix is from the upper right to the lower left. The strand determined to be interacting most closely with the helix is the second from the left, and this strand is parallel to both its neighbors. The Ω angle for this particular interaction is 120°.

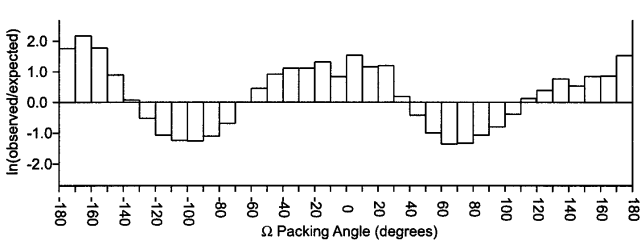

Figure 2. Distribution of helix–helix Ω packing angles.

Table 1. *Assigning a unique orientation value for each strand in a sheet*

Strand order	Orientation value	Total number of occurrences	Occurrences in reduced dataset	Correlation coefficient
⇵	−2	231	177	0.07
⇅	−1	367	247	−0.02
⇶	0	112	79	0.23
⇈	1	76	54	−0.25
⇈	2	140	91	−0.25

The left-hand column shows the strand for which we are computing an orientation value, depicted as a double-lined arrow, and its closest neighbor(s). Orientations −1 and 1 correspond to strands at the edge of a sheet. The values range from −2, most antiparallel, to +2, most parallel. The number of occurrences of helix–sheet packing arrangements observed for each strand orientation in the dataset of 1316 proteins is shown in the third column. Column four indicates the number of observed interactions for each strand type in the reduced dataset in which topologically constrained supersecondary structures were removed. The last column presents the correlation coefficients between local sheet twist and Ω packing angle for all five possible strand orientations in the total dataset, showing that the twist of the sheet does not correlate significantly with Ω. Thus, sheet twist is not sufficient to explain the observed helix–sheet Ω packing angle preferences.

Ω packing angle as a function of local sheet twist

To assess whether the trough formed by the natural twist in β-sheets influences the packing angle of helix–strand interactions, we plotted the relationship between local sheet twist angle and Ω. This was essentially a random scatter plot for all five strand orientations, showing no clear patterns. The correlation coefficients between local sheet twist and Ω angles were also small and variable in sign (Table 1). This indicates that packing angle preferences for antiparallel packing of helices against parallel regions of sheet cannot be explained based on sheet twist.

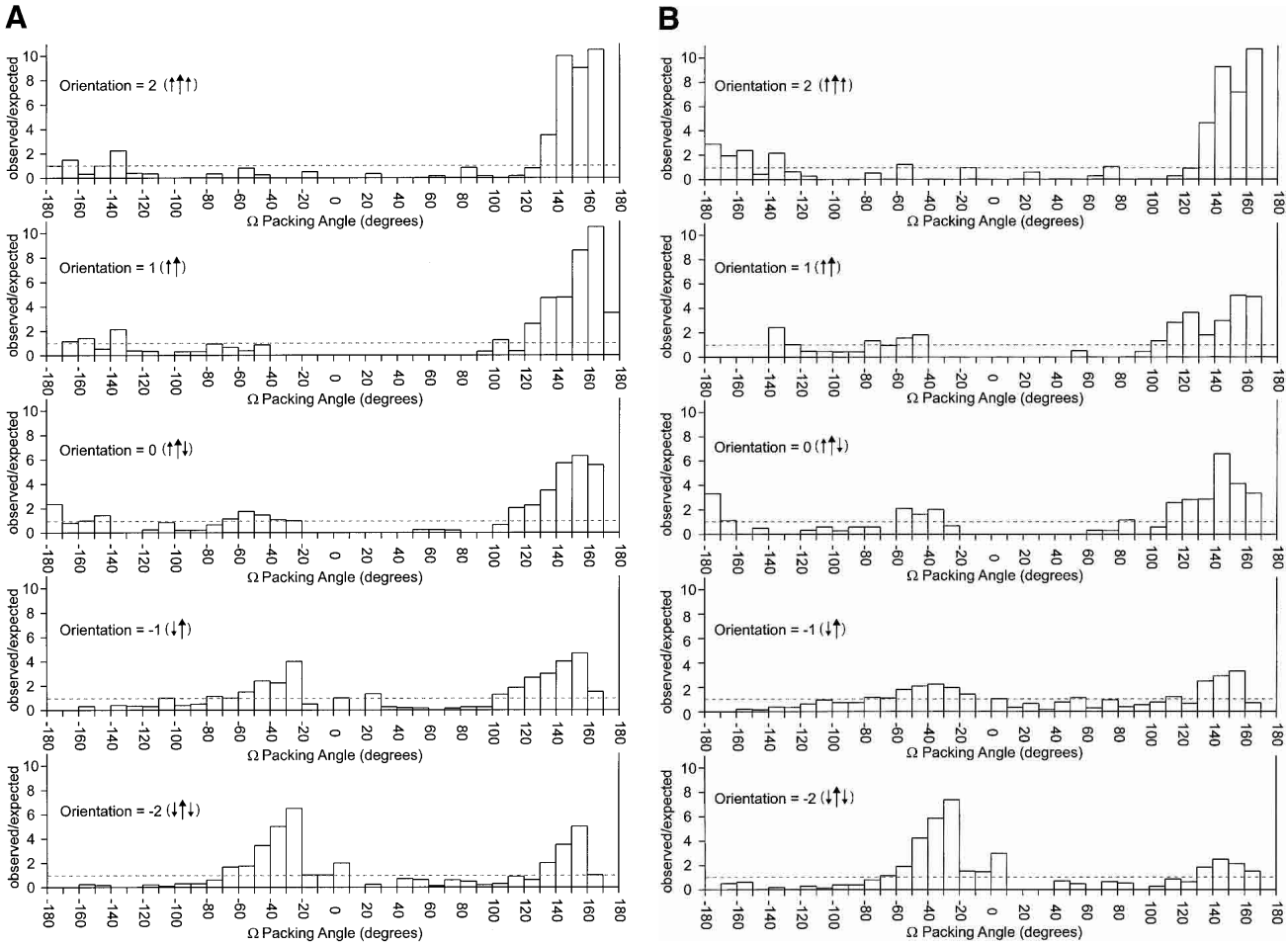

Figure 3. Distribution of helix–sheet Ω packing angles for each of the five strand orientations. A cartoon representation of the strand orientation is shown in the *upper left* of each histogram. The data are presented as the number of observed occurrences for each 10° bin, divided by the number expected from a uniform random distribution. A value of 1.0 (indicated by the gray dashed line) indicates that the range of observed Ω angles occurred just as often as expected. Values <1.0 are observed less often than expected, and values >1.0 indicate preferred packing angles. (*A*) Helix–strand pairs in which the strand has an orientation of 1 or 2 (parallel sheet) show a strong preference to pack antiparallel with the helix (Ω angles near 160°). Both parallel and antiparallel preferences in helix packing angle are observed when the strand has an orientation of −1 or −2 (antiparallel sheet). (*B*) Distribution of helix–strand Ω packing angles for each of the five strand orientations in which potential α-β supersecondary structures involving the interacting helix and strand have been removed from the dataset by disallowing helix–strand pairs that are consecutive in sequence.

Discussion

The distribution of helix–helix Ω packing angles (Fig. 2) strongly resembles that previously presented (Walther et al. 1998). These data indicate a sinusoidal trend in preferred Ω angles, with peaks corresponding to both parallel and antiparallel orientations and with few helices packed perpendicular to each other. Analyzing orientations in helix–sheet interactions is more complex, because an individual sheet can consist of all parallel, all antiparallel, or mixed parallel and antiparallel strands. This diversity in hydrogen bonding pattern, along with varying amino acid composition, also leads to nonplanarity being the rule, rather than the exception, for β-sheets. One hypothesis tested is that, as the twist of a sheet increasingly deviates from planarity, steric interactions between the helix and strands adjacent to the interacting strand would force the helix to turn, causing a stronger preference in Ω packing angle. However, no significant correlation was observed between local sheet twist and Ω packing angle. Thus, the observed preference for antiparallel alignment of helices with parallel regions of sheets could be due to dipole interactions between the helix and sheet, or local side-chain interactions being more important than sheet twist in defining the helix orientation. Side chains vary significantly in their interaction properties, and may also be flexible. Thus, an analysis of the role of side-chain interactions in helix–sheet packing, similar to that reported for helix–helix packing interfaces (Walther et al. 1996), is warranted.

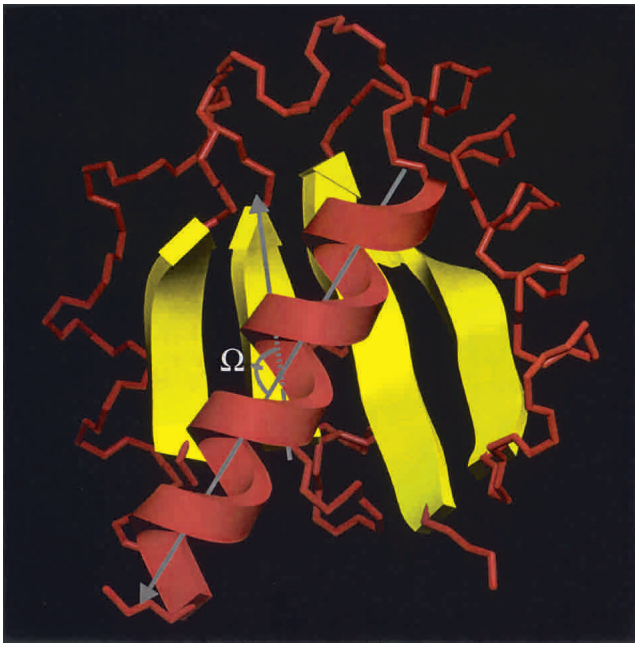

Figure 4. Example of an antiparallel helix–sheet packing interaction observed in the protein IIB cellobiose (PDB code: 1iib) from *Escherichia coli*. The geometry of the helix interaction was measured relative to the second strand from the *left*, which has an orientation value of 2 (parallel sheet). The yellow arrows, representing each strand, point in the N- to C-terminal direction. The N- to C-terminal direction of the helix is from *upper* right to *lower* left. The measured Ω angle is 120°, an antiparallel packing arrangement favored for parallel β-sheets.

In the distributions of Ω angle for each strand orientation shown in Figure 3, the orientations showing the strongest Ω angle preference are those in which the interacting strand is parallel to its neighbors. In these cases, strand orientations 1 and 2, the helix prefers to pack antiparallel to the strand, at an angle near 160°. One possible explanation for this preference is the presence of a net dipole arising from the hydrogen bonding pattern in parallel strands. The hydrogen bonds between antiparallel strands are nearly perpendicular to the protein backbone, and a negligible net dipole moment is produced. In these helix–strand interactions, the dipole would not be expected to play a role, and we observe no strong preference in Ω angles. However, hydrogen bonds between parallel strands make an ~20° angle with respect to the N-terminal to C-terminal direction of the protein backbone, leading to net dipole moment of about 1.15 Debyes (Hol et al. 1981). It was previously observed that there is a favorable electrostatic interaction energy between dipoles of helices and sheets in proteins consisting entirely of parallel sheets, indicating antiparallel packing of the structures would be favored (Hol et al. 1981). This trend for strong antiparallel preference in helix packing is observed in our study of helix–sheet interactions found in all the 1316 proteins.

It recently has been emphasized that the proteins comprising the PDB contain a significant number of repeated supersecondary structure motifs (Salem et al. 1999). Of particular importance to our study is the prevalence of the β-α-β supersecondary structure (Sternberg and Thornton 1976). This motif consists of two strands, hydrogen bonded in parallel, and connected by a stretch of protein that contains at least one helix. Often the loop region between one of the strands and the helix is short (≤7 residues), which forces the helix to pack antiparallel to the strand, as the loop region is not long enough to allow a parallel helix–strand interaction. An analysis of helix–strand interactions in which potential β-α-β motifs were excluded (Fig. 3B) yielded remarkably similar Ω angle distributions relative to the entire dataset (Fig. 3A). This similarity indicates that the preference for helices to pack antiparallel to parallel regions of sheets does not result from conformational restrictions imposed by short loops during folding.

In conclusion, the preferred packing angles found for helix–helix interactions support the results of earlier studies, whereas we uncover a significant preference for antiparallel packing between helices and strands that is strongly dependent on the degree of parallel content in the sheet. In addition to indicating a role for helix–sheet dipole interactions in guiding and stabilizing protein supersecondary structure formation, these preferred angles for helix–sheet packing can be useful guides for protein design.

Materials and methods

Protein dataset

The culled PDB list (Hobohm et al. 1993) from March 8, 2002 was used to create a dataset of protein crystal structures with <20% sequence identity, better than 2.2 Å resolution, and R-factors below 0.2. Only proteins whose PDB files contained HELIX and SHEET assignments were included. The final dataset consisted of 1316 proteins.

Representing secondary structures as vectors

The residues forming regular secondary structure in each PDB file were identified according to the HELIX and SHEET records. To include only significant interactions, we required helices to have at least seven residues, corresponding to two complete turns of a regular α-helix. Strands were required to have at least three residues for proper fitting of a vector to the C_α coordinates. Assuming a rise/residue of 1.5 Å for helices and 3.5 Å for strands, the minimal structures allowed for helices and sheets both have an axial length of 10.5 Å. For each sheet identified, the closest distance between neighboring strands was measured, and any sheet that had a closest interstrand distance >5.0 Å was visually checked to see that the strands were listed in the proper topological order. Errors in strand order within a PDB file were fixed manually.

The α-carbon positions of each residue in a helix and strand were used to compute the best-fit line through a given structure by using a parametric least squares algorithm (Christopher et al.

1996). Because an individual strand can deviate severely from linearity, the degree to which each strand bowed was also computed as: Bow = $\|\mathbf{m}\| / \|\mathbf{d}\|$, where **d** is a vector between the first C_α and the last C_α in the strand, and **m** is a perpendicular vector from **d** to the C_α in the middle of the strand. If the strand contained an even number of residues, the average position of the middle two C_α's was used to compute **m**.

Identifying a pair of interacting secondary structures

Each helix in a protein was represented in 3D by a finite axial vector **h**, and each strand, or second helix in the case of helix–helix interactions, was represented by a vector **s**, as shown graphically in Figure 1. The Euclidean distance between the midpoints of **h** and **s** was defined as *MD*. The closest point of approach between **h** and vector **s** was computed using equations described by Chothia et al. (1981). The quantity CP1 was defined as the percentage along the length of **h**, relative to its start, to reach the point closest to the vector **s**. Similarly, CP2 defines the percentage along vector **s** to reach the point closest to vector **h**. If both CP1 and CP2 were between 0.0 and 1.0, then the line of closest approach, represented by vector **L** (of length *CD*), would intersect the axis of both secondary structures.

A helix was defined as interacting with a strand if the following criteria were met:

1. Midpoint distance $MD \leq 20.0$ Å (a rough screen).
2. Closest distance $CD \leq 13.0$ Å (ensuring two structures interact closely).
3. $0.01 \leq$ CP1, CP2 ≤ 0.99 (ensuring that the closest point of interaction is within the secondary structure itself).
4. For helix–strand pairs only: $CD_j \leq 13.0$ Å; $CD_k \leq 13.0$ Å, where j and k are the two closest strands to **s** (ensuring the helix is interacting with the face of the sheet, not along the edge).
5. For helix–strand pairs only: The interacting strand and its neighboring strand(s) must have Bow ≤ 0.25 (ensuring that the sheet in the vicinity of a helix–strand interaction is not excessively bowed, because of β-bulges or nonstandard Φ, Ψ angles; Salemme 1983).

Assigning local strand orientation

The orientation of a strand relative to its hydrogen bonded neighbor(s) was determined using the "sense" field assigned to columns 39–40 of the SHEET record in a PDB file. The orientation value of strand *i* was computed as the sense of strand *i* plus the sense of strand *i* + 1. For example, if the second strand in a sheet is parallel to the first one, it has a sense value of 1. If the third strand in the sheet is parallel to the second strand, it also has a sense value of 1. The orientation value of the second strand is the sum of these two values, 1 + 1 = 2. Table 1 lists the five possible orientation values that can occur for a strand in a sheet, ranging from −2, most antiparallel, to +2, most parallel.

Measuring the Ω packing angle and local sheet twist

Because the vector of closest approach, **L**, is perpendicular to both **h** and **s**, the packing geometry between the two structures can be defined by a single dihedral angle, Ω. This angle is measured between **s** and the projection of **h** into the plane defined by **s** and $\mathbf{s} \times \mathbf{L}$ (Fig. 1).

The local sheet twist was measured to determine the extent to which the helix–sheet packing angle depends on steric interactions with the groove formed by the sheet, due to the twisting of its strands. For a helix–strand interaction, the orthogonal vectors **s** and **L** were used to describe a plane, *W*, that is locally perpendicular to the surface of the sheet. The vectors representing the two neighboring strands to **s** were then projected onto *W*. The sheet twist local to strand **s** was then computed as the average angle between strand **s** and the projection of each neighboring strand onto *W*. The sign of the twist angle corresponds to the expected increase or decrease in Ω angle due to steric effects as local sheet twist increases.

Helix–helix Ω packing angles

The distribution of helix–helix packing angles was measured to allow comparison to previous studies of secondary structure packing and to assess any changes in the distribution due to using a larger database of interactions. Identification and analysis of helix–helix packing were performed as described earlier for helix–sheet pairs, except that a second helix took the place of the strand. Bias in the distribution of observed helix–helix packing angles was removed as described previously (Walther et al. 1998).

Removing topologically constrained interactions from the dataset

To create a subset of the data in which topologically constrained interactions were removed, the order of the secondary structures along the primary structure of each protein was determined. The subset was created by excluding any helix–strand pair if the loop connecting them did not contain another secondary structure.

Normalizing the distributions of helix–sheet Ω angles

A geometric bias proportional to sinΩ, which arises because of finite length vector representations of the secondary structures, was taken into account as described previously (Walther et al. 1998). However, only a sinΩ correction was used, rather than $\sin^2\Omega$. A second sinΩ bias, due to the inequality of the solid angles arising from equal sampling of Ω in a spherical–polar distribution (Bowie 1997), for helix–helix pairs does not occur for helix–sheet interactions. This is because close packing requires that the helices lie roughly in a plane, rather than a spherical section, relative to the sheet.

Acknowledgments

We would like to acknowledge the support of the Center for Biological Modeling and an NIH Mathematics in Biology grant GM67249 toward this research. We also appreciate the helpful feedback of Prof. John Wilson during the early stages of this work.

The publication costs of this article were defrayed in part by payment of page charges. This article must therefore be hereby marked "advertisement" in accordance with 18 USC section 1734 solely to indicate this fact.

References

Baker, D. 2000. A surprising simplicity to protein folding. *Nature* **405:** 39–42.

Berman, H.M., Westbrook, J., Feng, Z., Gilliland, G., Bhat, T.N., Weissig, H., Shindyalov, I.N., and Bourne, P.E. 2000. The Protein Data Bank. *Nucleic Acids Res.* **28:** 235–242.

Bowie, J.U. 1997. Helix packing angle preferences. *Nat. Struct. Biol.* **4:** 915–917.

Bryngelson, J.D., Onuchic, J.N., Socci, N.D., and Wolynes, P.G. 1995. Funnels, pathways, and the energy landscape of protein folding: A synthesis. *Proteins* **21:** 167–195.

Chothia, C., Levitt, M., and Richardson, D. 1981. Helix to helix packing in proteins. *J. Mol. Biol.* **145:** 215–250.

Chou, K.-C., Nemethy, G., Rumsey, S., Tuttle, R.W., and Scheraga, H.A. 1985. Interactions between an α helix and a β sheet. *J. Mol. Biol.* **186:** 591–609.

Christopher, J.A., Swanson, R., and Baldwin, T.O. 1996. Algorithms for finding the axis of a helix: Fast rotational and parametric least-squares method. *Comput. Chem.* **20:** 339–345.

Cohen, F.E., Sternberg, M.J.E., and Taylor, W.R. 1982. Analysis and prediction of the packing of α-helices against a beta-sheet in the tertiary structure of globular proteins. *J. Mol. Biol.* **156:** 821–862.

Hespenheide, B.M., Rader, A.J., Thorpe, M.F., and Kuhn, L.A. 2002. Identifying protein folding cores from the evolution of flexible regions during unfolding. *J. Mol. Graph. Model.* **21:** 195–207.

Hobohm, U., Scharf, M., and Schneider, R. 1993. Selection of representative protein data sets. *Protein Sci.* **1:** 409–417.

Hol, W.G.J., Halie, L.M., and Sander, C. 1981. Dipoles of the α-helix and β-sheet: Their role in protein folding. *Nature* **294:** 532–536.

Honig, B. 1999. Protein folding: From the Levinthal paradox to structure prediction. *J. Mol. Biol.* **293:** 283–293.

Janin, J. and Chothia, C. 1980. Packing of α-helices onto β-pleated sheets and the anatomy of α/β proteins. *J. Mol. Biol.* **143:** 95–128.

Karplus, M. and Weaver, D.L. 1994. Protein folding dynamics: The diffusion-collision model and experimental data. *Protein Sci.* **3:** 650–668.

Kippen, A., Sancho, J., and Fersht, A.R. 1994. Folding of barnase in parts. *Biochemistry* **33:** 3778–3786.

Li, R. and Woodward, C. 1999. The hydrogen exchange core and protein folding. *Protein Sci.* **8:** 1571–1591.

Perrett, S., Clarke, J., Hounslow, A.M., and Fersht, A.R. 1995. Relationship between equilibrium amide proton exchange behavior and the folding pathway of barnase. *Biochemistry* **34:** 9288–9298.

Reddy, B.V.B. and Blundell, T.L. 1993. Packing of secondary structural elements in proteins. Analysis and prediction of inter-helix distances. *J. Mol. Biol.* **233:** 446–479.

Salem, G.M., Hutchinson, E.G., Orengo, C.A., and Thornton, J.M. 1999. Correlation of observed fold frequency with the occurrence of local structural motifs. *J. Mol. Biol.* **287:** 969–981.

Salemme, F.R. 1983. Structural properties of protein β-sheets. *Prog. Biophys. Mol. Biol.* **42:** 95–133.

Sternberg, M.J. and Thornton, J.M. 1976. On the conformation of proteins: The handedness of the β-strand-α-helix-β-strand unit. *J. Mol. Biol.* **105:** 367–382.

Udgaonkar, J.B. and Baldwin, R.L. 1988. NMR evidence for an early framework intermediate on the folding pathway of ribonuclease A. *Nature* **335:** 694–699.

van Montfort, R.L., Pijning, T., Kalk, K.H., Reizer, J., Saier Jr., M.H., Thunnissen, M.M., Robillard, G.T., and Dijkstra, B.W. 1997. The structure of an energy-coupling protein from bacteria, IIB cellobiose, reveals similarity to eukaryotic protein tyrosine phosphatases. *Structure* **5:** 217–225.

Walther, D., Eisenhaber, F., and Argos, P. 1996. Principles of helix-helix packing in proteins: The helical lattice superposition model. *J. Mol. Biol.* **255:** 536–553.

Walther, D., Springer, C., and Cohen, F.E. 1998. Helix-helix packing angle preferences for finite helix axes. *Proteins* **33:** 457–459.